Tunguska Meteor Fall of 1908: Effects on Stratospheric Ozone

R. P. Turco, O. B. Toon, C. Park
R. C. Whitten, J. B. Pollack, P. Noerdlinger

Summary. In 1908, when the giant Tunguska meteor disintegrated in the earth's atmosphere over Siberia, it may have generated as much as 30 million metric tons of nitric oxide (NO) in the stratosphere and mesosphere. The photochemical aftereffects of the event have been simulated using a comprehensive model of atmospheric trace composition. Calculations indicate that up to 45 percent of the ozone in the Northern Hemisphere may have been depleted by Tunguska's nitric oxide cloud early in 1909 and large ozone reductions may have persisted until 1912. Measurements of atmospheric transparency by the Smithsonian Astrophysical Observatory for the years 1909 to 1911 show evidence of a steady ozone recovery from unusually low levels in early 1909, implying a total ozone deficit of 30 ± 15 percent. The coincidence in time between the observed ozone recovery and the Tunguska meteor fall indicates that the event may provide a test of current ozone depletion theories.

On the morning of 30 June 1908, an immense meteor exploded over the Stony Tunguska River basin of Central Siberia (61°N, 102°E) with the force of a 10-megaton nuclear detonation (*1–4*). The scale of the meteor impact was unprecedented in recorded history. Two thousand square kilometers of ancient forest were blown flat, men 60 km from the fall site were thrown down and seared by the heat, the bolide was seen for hundreds of kilometers around, the explosion was heard for 1000 km, and the air wave disturbance circled the globe twice (*5, 6*). Although the nature of the Tunguska meteor has never been determined unequivocally, current ideas point to a small comet or cometary fragment (*7–10*). Studies of seismic and barometric records from 1908, coupled with the distinctive butterfly pattern of forest destruction, have been interpreted in terms of strong shock waves emanating from a large body flying supersonically at a relatively shallow angle (*2, 4, 8, 11*). The absence of impact craters or meteorite fragments of any substantial size suggests that the Tunguska object had an unusually low density and was stopped by the atmosphere, causing its complete disintegration (*11–13*).

Park (*12*) performed detailed aerodynamic simulations of the Tunguska meteor fall, utilizing the most probable trajectory parameters from previous investigations (*4, 5, 14, 15*) and a total intrinsic energy of the meteor approaching 4×10^{25} ergs. His calculations were consistent with earlier dynamical simulations. However, Park's model was unique in that he calculated the air chemistry in the wake of the meteor and, in particular, gave the production of nitric oxide (NO) in the heated air (*16*). For the most reasonable set of dynamical parameters, Park estimated that 30×10^6 metric tons (1 metric ton = 10^6 grams) of NO were deposited between 10 and 100 km (*17*), which is roughly five times the amount of odd nitrogen ($NO_x \equiv NO + NO_2 + HNO_3$) contained in the entire stratosphere of the earth (*18*). We have simulated the effect of such a large NO injection on the ambient ozone layer, and uncovered observational evidence for the effect.

R. P. Turco is a research scientist at R & D Associates, Marina del Rey, California 90291. O. B. Toon, C. Park, R. C. Whitten, and J. B. Pollack are physicists affiliated with the NASA Ames Research Center, Moffett Field, California 94035. P. Noerdlinger is an astrophysicist at Michigan State University, East Lansing 48824.

Photochemical Impact of the Tunguska Meteor

The research of Crutzen (*19*) and Johnston (*20*) provides the theoretical foundation for studying the ozone perturbations caused by large stratospheric NO_x injections. Recent developments in the theory are reviewed in (*21*). Tests of the NO_x-ozone theory have been sought in data on nuclear explosions (*22*) and solar proton events (*23*). In the first instance, the results were inconclusive, and in the second, although sizable ozone depletions were observed above 25 km, an effect on the total ozone column content was not detected. Accordingly, the Tunguska meteor fall may provide a novel test of the NO_x-ozone theory under highly perturbed conditions.

We employed a fully interactive one-dimensional photochemical model (*24*) to simulate the aftereffects of the Tunguska event. Previously, the model was applied to study ozone perturbations caused by massive NO injections following nuclear explosions (*25*). Here, the latest recommended chemical kinetic rate constants were utilized (*26*). For extremely large NO_x injections, the pertinent NO_x-O_x reaction cycle and rate coefficients have not changed significantly in recent years. A new rate constant for the reaction of OH with HNO_3 (*27*) has important consequences for the ambient partitioning of NO_x constituents (*27, 28*) and leads to a (somewhat) slower ozone recovery following a massive NO_x injection. Nevertheless, the effect is small with regard to the early ozone trend under investigation in this article.

Model predictions of ambient concentrations of ozone and other trace species were validated against observational data (*21*). The simulated stratospheric ozone profiles fall within the variability limits of the Krueger and Minzner (*29*) reference profile. The trace constituent distributions are also in generally satisfactory overall agreement with observations, although several specific points of disagreement exist (*21, 28*). The disparities imply uncertainty in the model calculations, as noted below.

For the present Tunguska simulations, the height profile of NO injection was taken from (*12*) and (*17*); the total NO injected was 3×10^7 metric tons. Water vapor, which may also be deposited by a cometary body, was found to have a negligible photochemical impact and is not considered further. Time-dependent calculations were made for three solar illumination conditions (30° latitude equinoctial and 50° latitude equinoctial and solstitial, each with a diurnal sun) and

 0036-8075/81/1002-0019$01.00/0

two spatial averagings of injected NO (the entire Northern Hemisphere, and a 10° latitude zone centered at 60°N—the latitude of the fall).

Figure 1 shows the time-dependent stratospheric ozone perturbations calculated for the Tunguska meteor fall. The hemispherically averaged model gives total stratospheric ozone reductions as large as 45 percent the first year, with significant reductions persisting for at least three more years (*30*). The Tunguska ozone depletions are comparable to those predicted for a nuclear war (*25*). At 40 km, ozone is quickly removed by photochemical reactions and does not begin to recover for a month. At 20 km, the ozone reduction becomes significant only after a delay of several weeks. This is due to the relatively slow chemical response of ozone in the lower stratosphere, where its ambient photochemical lifetime is at least several months. The ozone response at 30 km is intermediate between the responses at higher and lower altitudes. The structure in the 30-km ozone curve is due in part to the nonuniform initial injection profile of NO (see below). Relative to the air density, more NO is deposited at 50 km than at lower and higher altitudes. Thus some of the NO injected at 50 km diffuses downward and enhances the NO concentration at the 30-km level after a period of several months.

During the first month or two following the Tunguska event, it is more appropriate to estimate ozone depletions under the assumption that the injected NO was distributed over a limited latitude band. Results of such calculations corresponding to a 10° latitude zone are shown in Fig. 1. In this case, ozone above 10 km is found to be depleted by ~ 85 percent for several months. After 1 month, the ozone reductions at 20, 30, 40, and 50 km are 91, 93, 96, and 78 percent, respectively. In other words, the stratospheric ozone layer was essentially removed (locally) during this time span. Interestingly, the ozone column shows a more prompt onset of recovery in the zonal case than in the hemispheric case, apparently due to accelerated ultraviolet photodissociation of molecular oxygen following very rapid ozone depletion at all altitudes.

The odd nitrogen produced by the Tunguska meteor has two major sinks. The more important one is diffusion from the stratosphere to the troposphere, where it is efficiently washed out in rainfall, mainly in the form of HNO_3. There is, in addition, a photochemical sink for NO_x above 50 km, where the photolysis of NO creates N atoms, which react with NO to form N_2. The high-altitude odd nitrogen recombination process consumes roughly 20 percent of the injected NO.

The evolution of the ozone and total odd nitrogen height distributions following Tunguska are illustrated in Fig. 2. It can be seen that ozone is rapidly depleted above 40 km, but recovers quickly; below 30 km, ozone is slowly depleted, but the effects persist for several years (also see Fig. 1). As expected, the injected NO_x is eventually redistributed with a nearly uniform mixing ratio. The ozone profiles in Fig. 2 suggest that the Tunguska fall may have affected upper-atmospheric dynamics, inasmuch as absorption of ultraviolet sunlight by ozone is the major heat source for the stratosphere (*31*).

Uncertainties in the present photochemical model calculations arise from the uncertainty in the amount of NO injected by the Tunguska meteor [a factor of 2 to 3 according to (*12*) and (*17*)] and the numerous uncertainties associated with one-dimensional modeling (*21*). The ozone reductions corresponding to a given NO injection may be accurate within a factor of 2 after 1 year. They may be more uncertain for the first 1/2 year, when the horizontal extent of the spreading is unknown, and beyond 2 years, when removal and interhemispheric mixing rates and hydroxyl chemistry dominate the ozone perturbation.

Measurements of Atmospheric Transmission and Ozone Abundance

During the early 1900's, when the Tunguska meteor fell over Siberia, the Smithsonian Astrophysical Observatory (APO) was undertaking a long-term pro-

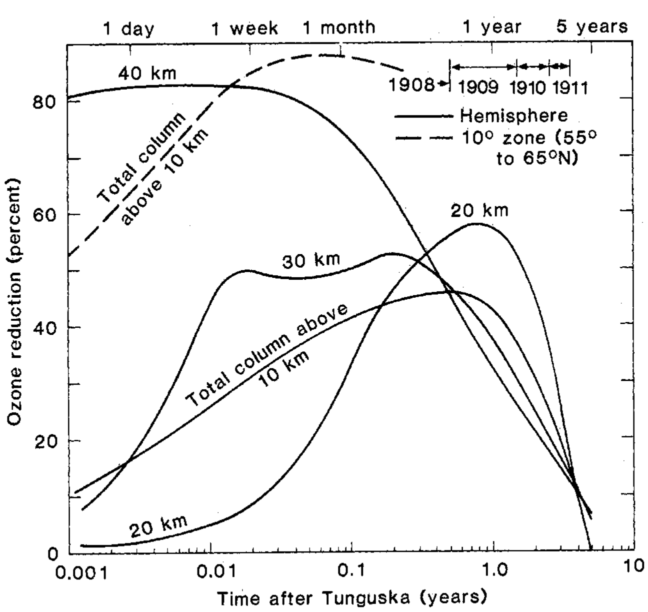

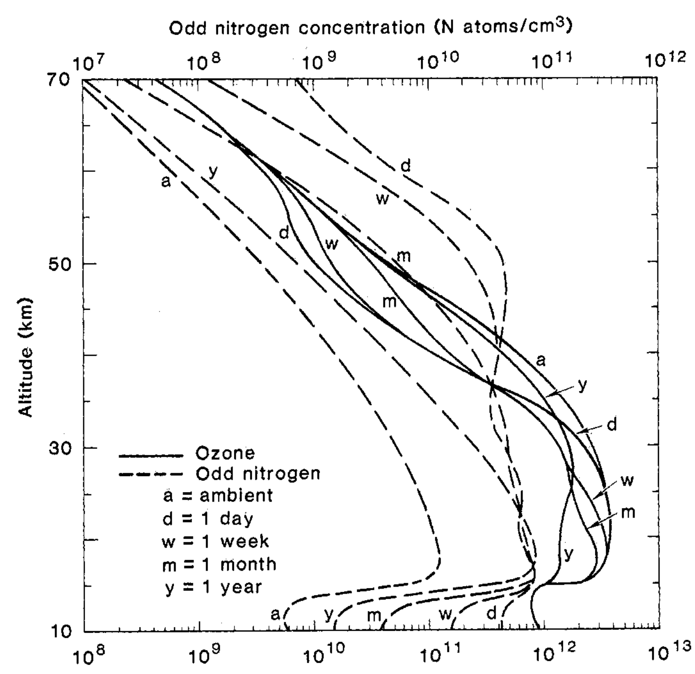

Fig. 1 (left). Ozone reductions predicted for the Tunguska meteor event. Decreases in ozone concentration at several altitudes and the total ozone reduction (in a vertical column above 10 km) are given. The model corresponds to 50°N equinoctial conditions. Two cases of initial horizontal spreading of the injected NO are depicted. The relative ozone reductions calculated for other conditions of solar illumination are similar to those illustrated. Fig. 2 (right). Calculated ozone and odd-nitrogen height profiles at various times after the Tunguska meteor fall. The results shown correspond to hemispheric spreading of the injected NO. The ozone concentrations are average daytime values for 50°N equinoctial conditions. Profiles for 30°N equinoctial conditions are similar.

gram to determine the variability of the solar constant (*32*). A spectrobolometer was used at Mount Wilson, California (34°N, 118°W), to determine the relative solar intensity between 0.35 and 1.6 micrometers. The spectra obtained were calibrated against simultaneous pyrheliometer observations. The absolute spectra were then analyzed as a function of solar zenith angle to determine the vertical transmission of the atmosphere at ten selected wavelengths in the range 0.35 to 1.6 μm. Data were collected only during half of each year (mid-spring to mid-fall), when viewing conditions at Mount Wilson were optimum.

In 1908 (and in subsequent years) the APO transmission record included data at three wavelengths (0.5, 0.6, and 0.7 μm) in the ozone Chappuis bands. The Chappuis bands are quite prominent in the atmospheric opacity spectrum. Angione *et al.* (*33*) exploited this fact to determine from the APO data base an ozone abundance record extending from 1912 to 1950, accurate on a daily basis to within 7 percent. Here, the APO data are used to calculate ozone column concentrations according to the relation

$$N_{O_3} = \frac{\tau_{0.6} - (\tau_{0.5} + \tau_{0.7})/2}{\sigma_{0.6} - (\sigma_{0.5} + \sigma_{0.7})/2} \qquad (1)$$

where N_{O_3} is the ozone column concentration (molecules per square centimeter), τ_λ is the optical depth at wavelength λ (micrometers) obtained from the APO record after subtraction of the molecular Rayleigh scattering component (*34*), and σ_λ is the ozone absorption coefficient (square centimeters) at wavelength λ. Equation 1 could not be applied to the 1908 data because the residual opacities (τ) were dominated by dust, due not only to the meteor impact but also to the eruption of the Russian volcano Shtyubelya Sopka in March 1907 (*17*). By 1909 the dust had been largely removed from the atmosphere by natural cleansing processes. Hence, subtraction of the average of the opacities at 0.5 and 0.7 μm from the opacity at 0.6 μm (Eq. 1) provided an effective means of eliminating the small background dust attenuation. In 1912 the Katmai eruption in Alaska again degraded the transmission data, and ozone retrievals were not attempted beyond 1911.

In determining ozone abundances from the APO data of 1909 to 1911, the clearest days were selected by requiring the overall solar transmission of the atmosphere (as designated in the APO records) to be greater than 83 percent (the transmission rarely exceeded 85 percent). Days for which the quality of the observations was judged to be less than "excellent" or "very good" (as determined by the Smithsonian workers) were ignored.

The day-to-day ozone concentrations for clear observational days above Mount Wilson between 1909 and 1911 are summarized in Fig. 3. For each year the corresponding average ozone concentration is also given, together with the standard deviation of the average concentration. The latter value is calculated by dividing the standard deviation, or scatter, of the individual data points by the square root of the number of observations. The substantial scatter in the ozone data arises mainly in the natural day-to-day variability of ozone, which can be attributed to the horizontal patchiness of the ozone overburden. Such variability is seen in all high-resolution measurements of the ozone column abundance (*33*). Nevertheless, the standard deviation of the mean of the data samples analyzed is relatively small, due to the large size of the samples available.

The observed trend in the ozone abundance from 1909 to 1911 is in close agreement with the model prediction for Tunguska, also shown in Fig. 3. (By 1909, the injected Tunguska NO would have been widely distributed over the Northern Hemisphere, and the hemispherically averaged model predictions of ozone change would be applicable.) Corrections for temperature feedback effects, interhemispheric mixing, and the known cyclic variations of ozone (diurnal, seasonal, quasi-biennial, and solar cycle) do not significantly alter the agreement in Fig. 3 (*17*). Thus the model prediction affords a reasonable fit to the data within 1 standard deviation.

A similar ozone analysis was conducted with other subsets of the APO data selected on the basis of the average transmission fraction and grade of observation. Restricting consideration to observations of higher apparent quality caused little change in the results, except that the statistics degenerated rapidly with the decreasing sample size. Including data of poorer quality in the analysis tended to bias the ozone toward larger average concentrations, while the trend of increasing ozone from 1909 to 1911 became less pronounced. Nevertheless, even the smallest subsets of data (which had large mean standard deviations) still suggested an increasing trend in ozone between 1909 and 1911.

To test further for the ozone trend, a linear regression analysis of the data in Fig. 3 was made. For the period from April 1909 to December 1911, the linear regression gave an absolute ozone in-

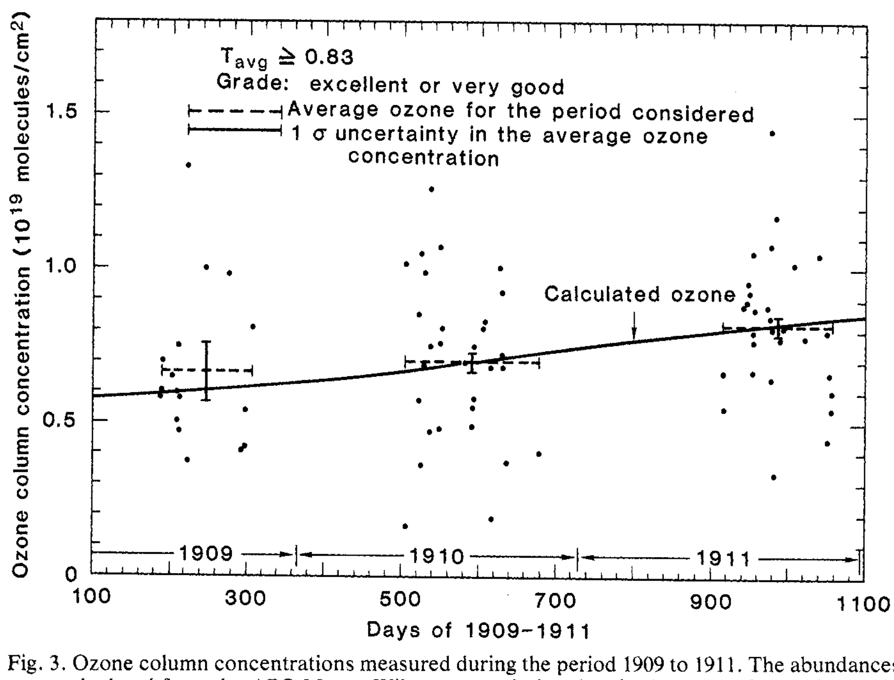

Fig. 3. Ozone column concentrations measured during the period 1909 to 1911. The abundances were calculated from the APO Mount Wilson transmission data in the ozone Chappuis bands. Each point gives the ozone abundance on a day of exceptional observational quality, as dictated by an average transmission fraction exceeding 83 percent and a high degree of measurement consistency (*32*). For each year, the mean ozone concentration and the standard deviation of the mean concentration are shown. Also plotted is the predicted total ozone variation from Fig. 1, after normalization to the observed 1910 ozone concentration (a small downward adjustment of less than 5 percent in the globally averaged ozone predictions for equinoctial conditions brings the measured and calculated amounts in 1910 into agreement). A correction to the model for the ozone content below 10 km—assuming 5×10^{17} ozone molecules per square centimeter between the elevation of Mount Wilson and 10 km—was also applied.

crease of $\sim 2.1 \times 10^{18}$ cm^{-2}, while the model calculations for Tunguska gave an average increase of $\sim 2.8 \times 10^{18}$ cm^{-2}. Because the ozone curve of growth is nonlinear, the regression line crudely represents the average rate of ozone increase at Mount Wilson during this period. The model simulations, on the other hand, define the recovery curve averaged over the entire hemisphere, but need to be adjusted for any specific location (*35*). By reasonable extrapolation of the computed regression line to an ambient ozone column abundance of $\sim 9 \times 10^{18}$ cm^{-2}, the analysis is compatible with an overall ozone reduction following Tunguska of 30 ± 15 percent at the 95 percent confidence level. This observational result, in combination with our independent theoretical estimates of the NO production and ozone depletion caused by the Tunguska meteor, may provide the first direct evidence that large total ozone depletions follow immense NO injections.

Implications of Tunguska

The diverse aeronomic effects of massive stratospheric NO_x injections have been studied by Reid *et al.* (*36, 37*), MacCracken and Chang (*38*), and Whitten *et al.* (*25*). The severe photochemical disturbances that attend such events can lead to changes in weather, climate, and solar ultraviolet flux at the ground. Similar phenomena may have been evident after the Tunguska event.

Weather records from the early 1900's were surveyed for possible climate and weather changes in the post-Tunguska era (*39, 40*). Several unusual weather conditions were found that appeared to commence around 1908 and persist for several years. For example, there was an increase (above a decreasing trend) in the south-to-north difference of the mean surface air temperature over North America (30° to 41°N) in both January and July beginning in 1909 and 1910. Total arctic sea ice increased rapidly between 1908 and 1911. In 1910 to 1915 the number of tropical cyclones of all intensities in the Atlantic Ocean and Caribbean Sea decreased by almost 50 percent from normal values, and remained unusually low for two decades.

A particularly interesting trend is the change in average surface temperatures of the Northern and Southern Hemispheres during this time. After 1908, and for almost a decade, the annual average surface temperature in the Northern Hemisphere (0° to 80°N) was decreasing, while the global and Southern Hemisphere (0° to 60°S) temperatures were increasing. In almost every other 10-year period from 1884 to 1974 all three temperatures had similar trends. The anomalous temperature difference represents an overall cooling of the Northern Hemisphere by about 0.2 to 0.3 K. However, the cooling may have been connected, in part, with the two large volcanic eruptions of that era at high northern latitudes—Shtyubelya Sopka (52°N) in 1907 and Katmai (58°N) in 1912. Each of these eruptions could have lowered the average temperature of the Northern Hemisphere by $\sim$ 0.4 to 0.8 K for about a year (*39*).

The response of tropospheric and stratospheric air temperatures to the Tunguska-generated changes in ozone, NO_x, and dust were calculated with the radiative transfer model of Pollack *et al.* (*41*). If the NO_2 and ozone perturbations occurring 1 and 2 years after the Tunguska meteor fall had persisted long enough to overcome the response time of the earth's climate system, then the predicted Northern Hemisphere surface coolings would have been 0.3 and 0.2 K, respectively. The Tunguska dust could have lowered the surface temperature another 0.05 K. These coolings are roughly one-half to one-third of those calculated for the two volcanic eruptions (*39, 41*). Because the ozone perturbations lasted for about 3 years, about one-half to two-thirds of the "steady-state" temperature changes might actually be expected to occur (similarly for the volcanoes). Inasmuch as the computed temperature changes for Tunguska are comparable to those associated with the volcanic eruptions of 1907 and 1912, they may be detectable through a rigorous analysis of the temperature record.

Predicted stratospheric temperature decreases associated with the Tunguska event were between 1 and 2 K. However, no data are available from the early 1900's with which to compare these predictions.

While a long list of apparent weather anomalies spanning a wide range of spatial and temporal scales can be identified during the Tunguska epoch, it is important to note that over this period most of the earth exhibited normal weather patterns, or deviations from normal patterns within the bounds of expected variability. Therefore, an unambiguous relation between the Tunguska meteor fall, large ozone depletions, and weather or climate changes cannot be established by the present analysis. An interesting side note, however, is that the combination of three large atmospheric disturbances between 1907 and 1912 (two large volcanoes and the Tunguska meteor fall) did not trigger a major climatic alteration; if anything, the observed climate changes were well within the bounds estimated from conventional theories.

Large ozone reductions, such as those calculated for the Tunguska event, can have severe environmental consequences. For example, a 45 percent ozone depletion can result in almost a tripling of the erythemally active ultraviolet radiation intensity at the ground (30°N, noontime, spring) (*42*). For smaller ozone reductions (for instance, $\sim$ 10 percent), the increase in radiation dosage is roughly twice the ozone decrease ($\sim$ 20 percent). The potential biological consequences of ultraviolet radiation enhancements are numerous, including a greater frequency of skin cancer in man and more pervasive destruction of sensitive plants and microorganisms. The actual impacts are not yet precisely known and are controversial. If the present ozone calculation for Tunguska is correct, however, the Northern Hemisphere may have received double the average normal amount of ultraviolet radiation from 1908 through 1911.

The great Tunguska meteor fall may have historical significance. We estimate that a cosmic body the size of Tunguska could strike the earth once each 1,000 to 20,000 years (*17*). On the time scale of 100 million years, much larger objects (asteroids and comets) can collide with our planet. Some of these massive objects, particularly comets, might interact strongly with the atmosphere, resulting in the formation of large quantities of NO. Dense swarms of high-velocity, moderate-sized meteoroids which penetrate deep into the stratosphere can also generate large quantities of NO (*43*). Exploding meteors (carbonaceous chondrites) are common even today. It follows that intense meteoric influxes in past epochs may have resulted in severe ozone depletions on a global scale lasting for up to 5 years. Two possible consequences of such large photochemical disturbances are a change in climate and an increase in ultraviolet radiation at the ground.

Alvarez *et al.* (*44*) recently uncovered a 20- to 160-fold enhancement in sedimentary iridium concentrations over a short time interval at the end of the Cretaceous period, which they interpreted as evidence of an impact by a large asteroid that threw dust into the stratosphere and disrupted the reptilian food chain. Their hypothesis is supported by

Ganapathy's discovery *(45)* of a similar pattern of enrichment of other noble metals in Cretaceous-Tertiary boundary clay. We point out that an intense influx of cometary fragments of the Tunguska type would have led to large ozone depletions worldwide. Detailed cratering simulations suggest that the observed meteoric-to-terrestrial mass ratio of the terminal Cretaceous clay and the absence of a large impact crater can be explained by a meteor shower or comet impact theory *(46)*. Alvarez *et al.* *(44)* fixed the mass of the postulated asteroid at more than 10^{11} metric tons—more than a factor of 10^5 times the estimated mass of the Tunguska meteor. Even if only 0.01 percent of the initial kinetic energy of a meteor this large were deposited in the atmosphere (assuming an entry velocity of $\gtrsim 20$ kilometers per second), a multi-Tunguska event would be expected.

Conclusion

We have investigated the possible ozone depletions associated with the Tunguska meteor fall of 1908. Ozone can be affected by the nitric oxide generated in the incandescent trail of a falling meteor. In the case of Tunguska, photochemical model calculations suggest a maximum ozone depletion (averaged over the Northern Hemisphere) of 35 to 45 percent. Archival atmospheric transmission data of the Smithsonian Astrophysical Observatory from the period of 1908 to 1911 have been analyzed for ozone Chappuis band absorption; the data imply an ozone reduction of $\sim 30 \pm 15$ percent. The Tunguska event is of interest in terms of its implications for ozone–odd nitrogen depletion theories, ozone-weather coupling hypotheses, and discontinuities in the geological record. To test these possibilities, a thorough analysis of data records from the Tunguska epoch is needed. The work reported here provides a starting point for such an analysis.

References and Notes

1. J. N. Hunt, R. Palmer, W. Penny, *Philos. Trans. R. Soc. London Ser. A* **252**, 275 (1960).
2. I. T. Zotkin and M. A. Tsikulin, *Sov. Phys. Dokl.* **11**, 183 (1966).
3. A. Ben-Menahem, *Phys. Earth Planet. Inter.* **11**, 1 (1975).
4. V. P. Korobeinikov, P. I. Chushkin, L. V. Shurshalov, *Acta Astronaut.* **3**, 615 (1976).
5. E. L. Krinov, *Giant Meteorites* (Pergamon, Oxford, 1966), pp. 125–265 and 383–387.
6. D. W. Hughes, *Nature (London)* **259**, 626 (1976).
7. F. J. W. Whipple, *R. Meteorol. Soc. J.* **56**, 287 (1930).
8. V. G. Fesenkov, *Soviet Astron.* **5**, 441 (1962); *ibid.* **10**, 195 (1966); *Solar System Res.* **3**, 177 (1969).
9. G. L. Wick and J. D. Isaacs, *Nature (London)* **247**, 139 (1974).
10. L. Kresak, *Bull. Astron. Inst. Czech.* **29**, 129 (1978).
11. G. I. Petrov and V. P. Stulov, *Cosmic Res. (USSR)* **13**, 525 (1975).
12. C. Park, *Acta Astronaut.* **5**, 523 (1978).
13. For detailed descriptions of the aerodynamic breakup mechanisms of large meteors, see B. Baldwin and Y. Sheaffer, *J. Geophys. Res.* **76**, 4653 (1971); Q. R. Passey and H. J. Melosh, *Icarus* **42**, 211 (1980).
14. I. T. Zotkin, *Meteoritika* **27**, 108 (1966).
15. V. A. Bronshten, *ibid.* **20**, 72 (1961).
16. The energy required to produce NO in a meteor trail is roughly 40 electron volts per NO molecule. Lightning requires about 50 eV, energetic subatomic particles about 35 eV, and nuclear explosions about 240 eV per NO molecule.
17. We have extended the aerodynamic calculations described in *(12)* and consider the nature of the Tunguska meteor and its aerodynamic properties, optical evidence for a dust cloud produced by the event, and the origin of the glowing skies seen after the fall.
18. E. Bauer, *J. Geophys. Res.* **84**, 6929 (1979).
19. P. J. Crutzen, *Q. J. R. Meteorol. Soc.* **96**, 320 (1970).
20. H. Johnston, *Science* **173**, 517 (1971).
21. R. D. Hudson and E. I. Reed, Eds., *The Stratosphere: Present and Future* (Reference Publication 1049, NASA, Washington, D.C., 1979).
22. J. S. Chang, W. H. Duewer, D. J. Wuebbles, *J. Geophys. Res.* **84**, 1755 (1979).
23. D. F. Heath, A. J. Krueger, P. J. Crutzen, *Science* **197**, 886 (1977).
24. R. P. Turco and R. C. Whitten, *Atmos. Environ.* **9**, 1045 (1975); *J. Atmos. Terr. Phys.* **40**, 13 (1978); *The NASA Ames Research Center One- and Two-Dimensional Stratospheric Models*, part 1, *The One-Dimensional Model* (Technical Paper 1002, NASA, Washington, D.C., 1977).
25. R. C. Whitten, W. J. Borucki, R. P. Turco, *Nature (London)* **257**, 38 (1975).
26. W. B. DeMore, L. J. Stief, F. Kaufman, D. M. Golden, R. F. Hampson, Jr., M. J. Kurylo, J. J. Margitan, M. J. Molina, R. T. Watson, *Chemical Kinetic and Photochemical Data for Use in Stratospheric Modelling* (Publication 81-3, Jet Propulsion Laboratory, Pasadena, Calif., 1981).
27. P. H. Wine, A. R. Ravishankara, N. M. Kruetter, R. C. Shah, J. M. Nicovich, R. L. Thompson, D. J. Wuebbles, *J. Geophys. Res.* **86**, 1105 (1981).
28. R. P. Turco, R. C. Whitten, O. B. Toon, E. C. Y. Inn, P. Hamill, *ibid.*, p. 1129.
29. A. J. Krueger and R. A. Minzner, *ibid.* **81**, 4477 (1976).
30. The lower boundary of the model is set at 10 km, and the calculated "total" ozone column density is essentially the stratospheric value. Tropospheric ozone contributes less than 10 percent to the total global ozone abundance. The behavior of tropospheric ozone for large stratospheric NO_x injections is not well understood. Accordingly, the low-altitude ozone component is neglected in this work.
31. In the present calculations the temperature feedback effects of ozone depletions are neglected. For large NO injections this may result in roughly a 10 percent overestimate of the ozone depletion [F. M. Luther, *Science* **192**, 49 (1976)]. The dynamical implications of large ozone reductions are not well established.
32. C. G. Abbot and F. E. Fowle, Jr., *Annals of the Astrophysical Observatory of the Smithsonian Institution* (Government Printing Office, Washington, D.C., 1908), vol. 2; C. G. Abbot, F. E. Fowle, L. B. Aldrich, *ibid.*, vol. 3.
33. R. J. Angione, E. J. Mederios, R. G. Roosen, *Nature (London)* **261**, 289 (1976).
34. The optical depth τ_λ and atmospheric transmission T_λ are related by $\tau_\lambda = -\ln(T_\lambda)$. The Rayleigh optical depth at Mount Wilson is specified by D. Deirmendjian, *Adv. Geophys.* **16**, 267 (1973).
35. The procedure for adjusting the ozone column is not obvious, but should probably include normalization to the local ozone concentration.
36. G. C. Reid, I. S. A. Isaksen, T. E. Holzer, P. J. Crutzen, *Nature (London)* **259**, 177 (1976).
37. G. C. Reid, J. R. McAfee, P. J. Crutzen, *ibid.* **275**, 489 (1978).
38. M. C. MacCracken and J. S. Chang, Eds., *A Preliminary Study of the Potential Chemical and Climatic Effects of Atmospheric Nuclear Explosions* (UCRL-51653, Lawrence Livermore Laboratory, Livermore, Calif., 1975).
39. H. H. Lamb, *Climate: Present, Past and Future*, vol. 1, *Fundamentals and Climate Now* (Methuen, London, 1972); *ibid.*, vol. 2, *Climatic History and the Future* (Methuen, London, 1977).
40. F. Exner, G. Walker, G. C. Simpson, H. H. Clayton, R. C. Mossman, *World Weather Records* (Publication 2913, Smithsonian Institution, Washington, D.C., 1944).
41. J. B. Pollack, O. B. Toon, C. Sagan, A. Summers, B. Baldwin, W. VanCamp, *J. Geophys. Res.* **81**, 1071 (1976); *J. Appl. Meteorol.* **15**, 247 (1976).
42. P. Cutchis, *Science* **184**, 13 (1974).
43. C. Park and G. P. Menees, *J. Geophys. Res.* **83**, 4029 (1978).
44. L. W. Alvarez, W. Alvarez, F. Asaro, H. V. Michel, *Science* **208**, 1095 (1980).
45. R. Ganapathy, *ibid.* **209**, 921 (1980).
46. J. D. O'Keefe and T. J. Ahrens, *Eos* **61**, 1021 (1980).

47. We thank C. A. Riegel, F. E. Volz, R. J. Angione, F. R. Gilmore, M. V. Wright, and J. T. Moore for helpful discussions. This work was partly supported by NASA contract NAS2-9881.